

Electromagnetic interaction of low transverse momentum electrons and positrons with heavy nuclei in ultra-peripheral ultra-relativistic heavy-ion collisions

Katarzyna Mazurek^{1*}, Mariola Klusek-Gawenda^{1†}
and Antoni Szczurek^{1,2†}

^{1*}, Institute of Nuclear Physics Polish Academy of Sciences,
Radzikowskiego 152, Kraków, PL-31342, , Poland.

²College of Natural Sciences, Institute of Physics, University of
Rzeszów, Pigoń 1, Rzeszów, PL-35310, , Poland.

*Corresponding author(s). E-mail(s):

Katarzyna.Mazurek@ifj.edu.pl;

Contributing authors: Mariola.Klusek-Gawenda@ifj.edu.pl;

Antoni.Szczurek@ifj.edu.pl;

[†]These authors contributed equally to this work.

Abstract

The photon-photon interaction in ultra-relativistic heavy-ion collision is a source of the (e^+, e^-) pairs. The photon-photon fusion leads the lepton creation in the broad configuration space around "collision" point. Those created close to heavy nuclei may undergo strong electromagnetic interaction with them. The impact parameter space distribution of electrons and positrons are calculated within the b-space EPA model of such collisions. The evolution due to the electromagnetic final state interaction (FSI) of (e^+, e^-) with nuclei is studied, and the distortion of rapidity and transverse momentum distributions are shown. Part of the analysis is independent of the production model. We show first exploratory results for the reaction Pb+Pb at $\sqrt{s_{NN}} = 17.3$ GeV (SPS) and 200 GeV (RHIC) energies. We provide results for selected creation points and when integrating over their position as dictated by the **b**-space EPA model. We observe a strong influence at low transverse momenta, so far not measured regions of the

phase space. In particular, we predict a possible sizeable accumulation of electrons with rapidities close to the beam rapidity. The EM effects lead to asymmetry in the production of electrons and positrons.

Keywords: keyword1, Keyword2, Keyword3, Keyword4

1 Introduction

Heavy-ion collisions are excellent factory for producing both elementary and composed particles as well as for studying their properties and production mechanism. Since many years efforts of theorists and experimentalists were focused on the investigation of time-space evolution of the quark-gluon plasma (QGP) and production of different species of particles, primarily hadrons (pions, kaons, nucleons, hyperons, etc.) emitted in the collision. At high energies, the velocities of such beam nuclei are close to light velocity thus they are often called ultra-relativistic velocities (URV).

Central collisions are the most interesting in the context of the QGP studies. Plasma is, of course, also produced in more peripheral collisions. In peripheral collisions, the so-called spectators are relatively large and have large moving charge. It was realized relatively late that this charge generates strong quickly changing electromagnetic fields that can influence the trajectories and some observables for charged particles.

Such effects were investigated in previous studies of one of the present authors [1, 2]. On one hand side the EM effects strongly modify the Feynman x_F spectra of low- p_T pions, creating a dip for π^+ and an enhancement for π^- at $x_F \approx \frac{m_\pi}{m_N}$. In [1] a formalism of charged meson evolution in the EM field (electric and magnetic) of fast moving nuclei was developed. Later on the spectacular effects were confronted with the SPS data [3] confirming the theoretical predictions. The investigation was done for $^{208}\text{Pb}+^{208}\text{Pb}$ at 158 GeV/nucleon energy ($\sqrt{s_{NN}} = 17.3$ GeV) at CERN Super Proton Synchrotron (SPS) [4]. In [2] the influence of the EM fields on azimuthal flow parameters (v_n) was studied and confronted in [5] with the RHIC data. It was found that the EM field leads to a split of the directed flow for opposite e.g. charges. In the initial calculation, a simple model of single initial creation point of pions was assumed for simplicity. More recently, such a calculation was further developed by taking into account also the time-space evolution of the fireball, treated as a set of firebreaks [6]. The distortions of the π^+ and π^- distributions allow to discuss the electromagnetic effects of the spectator and charged pions in URV collisions of heavy ions and nicely explain the experimental data. This study was done for non-central collisions where the remaining after collision object, called 'spectator', loses only a small part of nucleons of the original beam/target nucleus.

The ultra-peripheral collisions of heavy ions (e.g. $^{208}\text{Pb} + ^{208}\text{Pb}$) at ultra-relativistic energies ($\sqrt{s_{NN}} \geq 5$ GeV) [7] allow to produce particles in a broad

region of impact parameter space, even far from “colliding” nuclei. The nuclei passing near one to each other with ultrarelativistic energies are a source of virtual photons that can collide producing e.g. a pair of leptons. In real current experiments (RHIC, LHC), the luminosity is big enough to observe e.g. $AA \rightarrow AA\rho^0$ and $AA \rightarrow AAe^+e^-$, $AA \rightarrow AA\mu^+\mu^-$ processes. One of the most interesting phenomena is multiple interaction [7, 8] which may lead to the production of more than one lepton pair.

The studies on the creation of positron-electron pairs started in early 1930’ties with prediction of positron by Dirac [9], experimental discovery of positron by Anderson [10] and works of Breit and Wheeler [11], where they calculated the cross section for the production of such pairs in the collisions of two light quanta. The production of e^+e^- pairs in nucleus-nucleus collisions, goes back to the work on Bethe, Heitler [12] and Landau, Lifschitz [13] in 1934. It was Williams who realized [14] that the production of e^+e^- pairs is enhanced in the vicinity of the atomic nucleus. An overview of the theoretical investigation of the e^+e^- pairs creation in historical context was presented by e.g. Hubbell [15] and the detailed discussion about this process in physics and astrophysics was written by Ruffini et al. [16].

The early analyses were done in the momentum space and therefore did not include all details in the impact parameter space. An example of the calculation where such details are taken into account can be found e.g. in [7, 17]. In ultra-peripheral collision (UPC), the nuclei do not collide without losing, in principle, any nucleon. However, the electromagnetic final state interaction (FSI) induced by fast moving nuclei may cause excitation of the nuclei and subsequent emission of different particles, in particular neutrons [18] that can be measured both at RHIC and at the LHC. Moreover the UPC are responsible not only for Coulomb excitation of the spectator but also for the multiple scattering and production of more than one dielectron pair [8]. With large transverse momentum cut typical at RHIC and the LHC the effect is not dramatic.

New experimental results have shown that the b -space EPA may be not sufficient to describe some observables [19], such as $p_{t,pair}$ distribution. Very recently experimental results for the semi-central collisions controlled by centrality measurement have shown a strong enhancement at $p_{t,pair} \sim 0$ (STAR) [20] and a bump at small acoplanarity (ATLAS) [21, 22]. Inclusion of transverse momentum dependent photon distributions improved the situation [23] but did not give the observed experimentally dependence on impact parameter. Recently several works addressed the issue of impact parameter – transverse momentum correlations [24–27] for different interesting observables. A full treatment is a bit difficult [28] but gives very good description of the semi-central collision data.

Can the strong EM fields generated at high energies modify the electron/-positron distributions? No visible effect was observed for electrons with $p_T > 1$ GeV as discussed in [8], where the ALICE distributions were confronted

with the b -space equivalent photon approximation (EPA) model. But the electromagnetic effect is expected rather at low transverse momenta. According to our knowledge this topic was not discussed in the literature. As the spectators, which in ultra-peripheral collisions are almost identical to colliding nuclei, are charged, they can interact electromagnetically with electrons and positrons as it was in the case of pions. Similar effects as observed for pions may be expected also for charged leptons. The motion of particles in EM field depends not only on their charge but also on their mass. Thus the distortions of e^+/e^- distributions should be different than those for π^+/π^- distributions. Also the mechanism of production is completely different. In contrast to pion production, where the emission site is well localized, the electron-positron pairs produced by photon-photon fusion can be produced in a broad configuration space around the “collision” point - point of the closest approach of nuclei. A pedagogical illustration of the impact parameter dependence can be found e.g. in [17].

From one side, the previous works [6] and reference therein, were connected with the electromagnetic effects caused by the emission of the pions from the fireball region. From the other side, the model considered [17, 29, 30] can correctly estimate the localization in the impact parameter space. The present study will be focused on electromagnetic interaction between electrons/positrons with highly positively charged nuclei.

Our approach consists of two steps. First, the e^+e^- distributions are calculated within EPA in terms of initial distributions in a given space point and at a given initial rapidity and transverse momentum. Secondly, the space-time evolution of leptons in the electromagnetic fields of fast moving nuclei with URV is performed by solving relativistic equation of motion [31].

In Section 3 the details of the calculation of the differential cross section of e^+e^- production will be presented. We will not discuss in detail equation of motion which was presented e.g. in [31]. The results of the evolution of electrons/positrons in the EM field of “colliding” nuclei are presented in Section 4.

2 A comment on quantum multiple-photon exchange effects

The electromagnetic interaction of charged leptons with nuclei was discussed in many contexts in the literature. Very similar to the considered here process is $\gamma A \rightarrow l^+ l^- A$ reaction. The respective Coulomb effect was discussed e.g. in [32–35].

The history started with the seminal work of Bethe and Maximon [32]. They discussed the Coulomb effects for bremsstrahlung and dilepton pair production. Tuchin considered [34] multiple t -channel photon exchanges within the Glauber model. Ivanov and Melnikov [33] presented impact representation of the amplitude for e^+e^- photoproduction in the Coulomb field of the nucleus. They wrote leading amplitudes for N t -channel exchanges and showed that in

their approximations the amplitudes can be resummed. They calculated corrections to the total $\gamma A \rightarrow l^+ l^- A$ cross section which is of course much simpler than for differential distributions (not discussed there).

Very recently the Shandong group [35] discussed how to modify the TMD photon distributions in the nucleus due to strong Coulomb field of the nucleus. This approach may be relevant for $A(e, e' l^+ l^-) A$ at EIC and EicC. Also, this approach is not very useful in our case, where we need rather impact parameter formulation than momentum space formulation.

Very closely related are Coulomb effects in $\mu + A \rightarrow \mu + A + e^+ e^-$ [36–38]. In [37] the authors discuss distributions in $x = \epsilon_-/\omega$, where ϵ_- is electron energy and ω is initial photon energy. In a recent paper [38] the authors discuss distributions in $x = \epsilon_+/\omega$, where ϵ_+ is positron energy and distribution in muon energy loss through pair production relevant for muons propagating in the atmosphere.

The $AA \rightarrow AA l^+ l^-$ reaction was also discussed in the literature [39–48]. In Fig.1 we show an example of the amplitude for a few photon exchanges. It becomes obvious that resummation with exact kinematics and extended charges of nuclei is not easy.

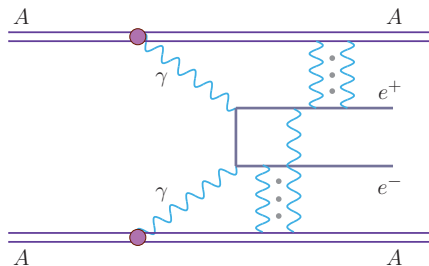


Fig. 1 An example of diagrams relevant for multi-photon exchanges.

The Massachusetts group discussed time-dependent two-center Dirac equation with Coulomb interaction [39, 40]. The papers have rather technical character. Neither quantitative predictions were given nor differential distributions were discussed.

The Frankfurt group [41] discussed how to modify the impact parameter dependent photon distributions in the strong electromagnetic field of the nuclei. As stated by the authors their approach is not adequate when lepton velocities are similar to the velocity of one of the nuclei. In the present paper we wish to discuss exactly this region of the phase space. The classical approach performed in [1, 6] for charged pion production in heavy ion collisions suggests that this is the region where spectacular effects may occur.

The authors of [48] reported an explicit calculation of the contribution of exchange of two photons from one nucleus and two photons from the other

nucleus. Their results suggest that the familiar eikonalization of Coulomb distortions breaks down. Some relations to $n\gamma + m\gamma \rightarrow l^+l^-$ were discussed there. A full formalism is not ready for practical calculations.

The short summary is intended to show that there is no ready formalism which can be used to calculate Coulomb modifications of differential distributions of individual, positively or negatively charged, leptons. Therefore in the following we suggest to use rather existing classical approach which seems much easier to apply for our purpose. We shall return to the discussion of this approach in the following sections.

3 Lepton pair production, equivalent photon approximation

The particles originated from photon-photon collisions can be created in full space around excited nucleus thus first of all the geometry of the reaction should be defined.

In the present study, the ultra-peripheral collisions (UPC) are investigated in the reaction plane (b_x, b_y) which are perpendicular to the beam axis taken as z -direction.

The collision point $(b_x = 0, b_y = 0)$ is time-independent center of mass (CM) of the reaction as shown in Fig. 2. The impact parameter is fixed as double radius of each (identical) Pb nucleus $b=(13.95 \text{ fm}, 14.05 \text{ fm})$. For comparison we will show results also for $b=(49.95 \text{ fm}, 50.05 \text{ fm})$.

Four characteristic points $(\pm 15 \text{ fm}, 0)$, $(0, \pm 15 \text{ fm})$, which are discussed later are also marked in the figure. In the present paper we shall show results for these initial emission points for illustrating the effect of evolution of electrons/positrons in the EM field of nuclei.

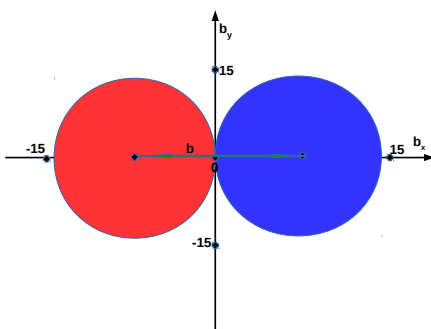


Fig. 2 The impact parameter space and the five selected points (b_x, b_y) : $(0, 0)$, $(\pm 15 \text{ fm}, 0)$, $(0, \pm 15 \text{ fm})$, for which the distribution in rapidity and transverse momentum will be compared latter on in the text, shown in the CM rest frame.

Here we wish to present some preliminary results for selected values of impact parameter. Till recently the b -space EPA [49] was state of the art

[50–52] for calculating dilepton production cross section, although a slightly different approach, with impact parameter - lepton momentum correlations, was available [53, 54]. Usually the exclusive dilepton production was estimated by using the monopole charge form factor which allows to reproduce correctly the total cross section. The differential cross sections are more sensitive to details, thus realistic charge form factor (Fourier transform of the charge distribution) has to be employed.¹ In the b -space EPA (see [49]) the total cross section for l^+l^- pair production via photon-photon fusion reads

$$\sigma = \int \frac{d\omega_1}{\omega_1} \int \frac{d\omega_2}{\omega_2} N(\omega_1, \mathbf{b}_1) N(\omega_2, \mathbf{b}_2) \Theta(b - R_1 - R_2) \times 2\pi \int_{R_1}^{\infty} b_1 db_1 \int_{R_2}^{\infty} b_2 db_2 \int_0^{2\pi} d\phi \sigma_{\gamma\gamma}(\omega_1, \omega_2). \quad (1)$$

This can be written in the equivalent way as [17]

$$\sigma_{AA \rightarrow AAe^+e^-} = \int \frac{d\sigma_{\gamma\gamma \rightarrow e^+e^-}(W_{\gamma\gamma})}{d\cos\theta} N(\omega_1, \mathbf{b}_1) N(\omega_2, \mathbf{b}_2) S_{abs}^2(\mathbf{b}) \times 2\pi b db d\bar{b}_x d\bar{b}_y \frac{W_{\gamma\gamma}}{2} dW_{\gamma\gamma} dY_{e^+e^-} d\cos\theta. \quad (2)$$

where $N(\omega_i, b_i)$ are photon fluxes, $W_{\gamma\gamma} = M_{e^+e^-}$ is invariant mass and $Y_{e^+e^-} = (y_{e^+} + y_{e^-})/2$ is rapidity of the outgoing system and θ is the scattering angle in the $\gamma\gamma \rightarrow e^+e^-$ center-of mass system. The gap survival factor S_{abs}^2 assures that only ultra-peripheral reactions are considered.

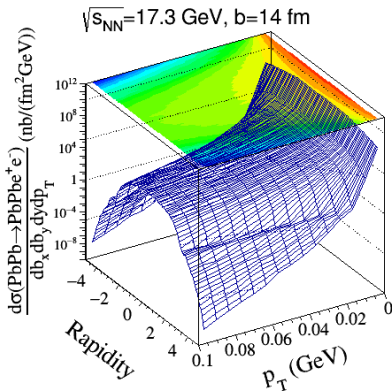


Fig. 3 The map of differential cross section in rapidity of electron or positron and lepton transverse momentum for $(b_x, b_y) = (0, 0)$ which will be called CM point for brevity.

¹Double scattering production of positron-electron pairs using the realistic charge form factor has been discussed in [7] and [8].

The $\bar{b}_x = (b_{1x} + b_{2x})/2$ and $\bar{b}_y = (b_{1y} + b_{2y})/2$ quantities are particularly useful for our purposes. We define $\vec{b} = (\vec{b}_1 + \vec{b}_2)/2$ which is (initial) position of electron/positron in the impact parameter space. This will be useful when considering motion of electron/positron in the EM field of nuclei. The energies of photons are included by the relation: $\omega_{1,2} = W_{\gamma\gamma}/2 \exp(\pm Y_{e^+e^-})$. In the following for brevity we shall use b_x, b_y instead of \bar{b}_x, \bar{b}_y . Then (b_x, b_y) is the position in the impact parameter plane, where the electron and positron are created.² The differential (in rapidity and transverse momentum) cross section could be obtained in each emission point in the impact parameter space (b_x, b_y) . The transverse momentum distribution of e^+ or e^- can be obtained by binning in Eq. (2) $p_t = p^* \sqrt{1 - \cos^2 \theta}$ where p^* is lepton momentum in the e^+e^- CM system. Similar binning is done for y_{e^+} and y_{e^-} .

The simple b -space EPA formula (2) gives good description of dielectron invariant mass distributions [7] as measured by the ALICE collaboration [55] for $p_{t,e} > 2$ GeV. Small electron/positron transverse momenta were not measure so far. In this approach the $p_{t,pair}$ and acoplanarity distributions are Dirac delta functions. In general, this approach allows to describe rather single lepton distributions (rapidity, transverse momentum). Below we shall compare a transverse momentum distribution of electrons of the b -space EPA with its counterpart for the Wigner-function approach [28] for a given range of impact parameter, relevant for the discussion in the present paper.

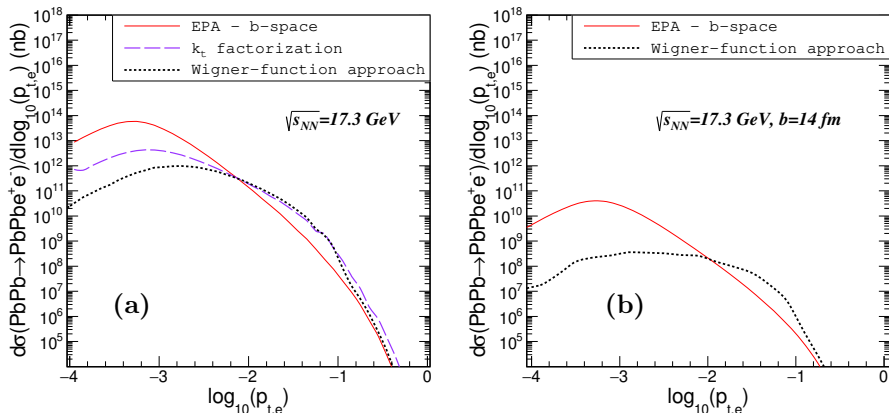


Fig. 4 Differential cross section for $\text{PbPb} \rightarrow \text{PbPb} e^+ e^-$ as a function of $\log_{10}(p_{t,e})$. Shown are results of different approaches as explained in the figure legend. The left panel shows impact parameter integrated cross section while the right panel is for a narrow range of impact parameter $b \in (13.95, 14.05)$ fm.

Can the subtle impact parameter – lepton transverse momentum correlations influence the single lepton transverse momenta? This was not discussed

²Expression (2) allows to estimate not only the lepton pair production but also a production of any other particle pair [17].

so far in the literature. In Fig. 4 we compare results for the somewhat simplified b -space EPA, the k_t -factorization approach [23] and the Wigner-function approach [28]. We show results for the full range of impact parameter (left panel) and well as for very limited range discussed in the present paper (right panel). In the latter case there is no k_t -factorization result shown in the left panel. We see interesting results for $p_{t,e} < 0.01$ GeV. This region requires dedicated studies in the context of possible measurement with ALICE3 detector. We observe deviations of the b -space EPA result and the Wigner-function approach result for small lepton transverse momenta $p_t < 0.1$ GeV. Sizeable numerical fluctuations in the Wigner-function approach can be observed. Since in the present exploratory calculations we are interested rather in estimating the size of the outcome related to the electromagnetic final state interactions (FSI) of leptons with the nuclei as well as phase-space localization (rapidity, transverse momentum) of the new FSI effect, in the present paper we wish to use a more handy b -space EPA approach (6-dimensional integration). One has to have in mind that precise evaluation of the low- p_t distributions requires use of the rather complicated Wigner-function approach (10-dimensional integration). Using the Wigner-function approach together with the inclusion of the final state interaction effects goes beyond the scope of the present paper but would not change the general conclusions drawn here.

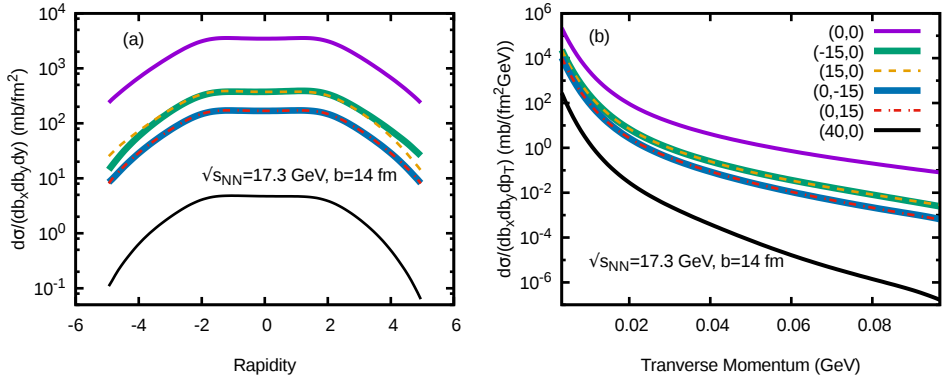


Fig. 5 (Color on-line) The differential cross section for various emission points of electron-positrons produced in the $^{208}\text{Pb}+^{208}\text{Pb}$ reaction at 158 GeV/nucleon energy ($\sqrt{s_{NN}} = 17.3$ GeV) at impact parameter 14 ± 0.05 fm. The cross section for selected points (b_x, b_y) : (0, 0), (±15 fm, 0), (0, ±15 fm) and (40 fm, 0) are integrated over p_T (a) and rapidity (b), respectively.

The calculations will be done assuming the collision of $^{208}\text{Pb}+^{208}\text{Pb}$ at 158 GeV/nucleon energy ($\sqrt{s_{NN}} = 17.3$ GeV) corresponding to the CERN SPS and $\sqrt{s_{NN}} = 200$ GeV of the STAR RHIC at impact parameter 14 ± 0.05 fm which is approximately twice the radius of the lead nucleus. This is minimal configuration assuring ultra-peripheral collisions.

Figure 3 illustrates the differential cross section on the plane of rapidity (y) vs. transverse momentum (p_T). Rather broad range of rapidity $(-5, 5)$ is chosen, but the distribution in p_T will be limited to $(0, 0.1 \text{ GeV})$ as the cross section drops at $p_T = 0.1 \text{ GeV}$ already a few orders of magnitude. The electromagnetic effects may be substantial only in the region of the small transverse momenta.

Thus for our exploratory study here we have limited the range for rapidity to $(-5, 5)$ and for transverse momentum to $p_T = (0, 0.1 \text{ GeV})$. The integrated distribution can be seen in Fig. 5(a) and (b). There we compare the distributions obtained for different emission points (b_x, b_y) : $(0, 0)$, $(\pm 15 \text{ fm}, 0)$, $(0, \pm 15 \text{ fm})$ as shown in Fig. 2. The behavior of the differential cross section is very similar in each (b_x, b_y) point but it differs in normalization as it is shown in Fig. 5.

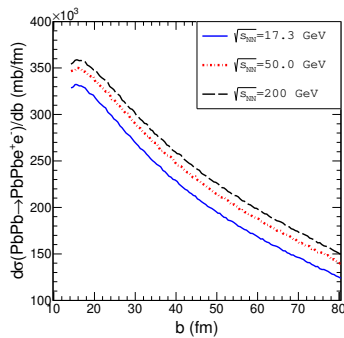


Fig. 6 Distribution of the cross section in the impact parameter b for different energies: $\sqrt{s_{NN}} = 17.3, 50$ and 200 GeV (from bottom to top).

In Fig. 6 we show a distribution of the cross section in impact parameter b for different collision energies $\sqrt{s_{NN}} = 17.3, 50, 200 \text{ GeV}$. In this calculation we have taken $p_T > 0 \text{ GeV}$ (the cross section strongly depends on the lowest value of lepton transverse momentum p_T). In general, the larger collision energy the broader the range of impact parameter. However, the cross section for $b \approx R_{A_1} + R_{A_2}$ is almost the same. Only taking into account limitation, e.g. on the momentum transfer, makes the difference in the cross section significant even at $b = 14 \text{ fm}$.

The emission point of the electrons/positrons does not change the behavior (shape) of the cross section on the (y, p_T) plane but changes the absolute value of the cross section. As it is visible in Fig. 5 (a) and (b) the biggest cross section is obtained for the CM emission point. The production of e^+, e^- at $(b_x, b_y) = (40 \text{ fm}, 0)$ i.e. far from the CM point, is hindered by three orders of magnitude. Moreover, the production at $b_x = \pm 15 \text{ fm}$ and $b_y = 0$ is more preferable than the production at $b_x = 0$ and $b_y = \pm 15 \text{ fm}$ what is fully understandable taking into account the geometry of the system (see Fig. 2). As the system taken here into consideration is fully symmetric ($A_1 = A_2, Z_1 = Z_2$), thus corresponding

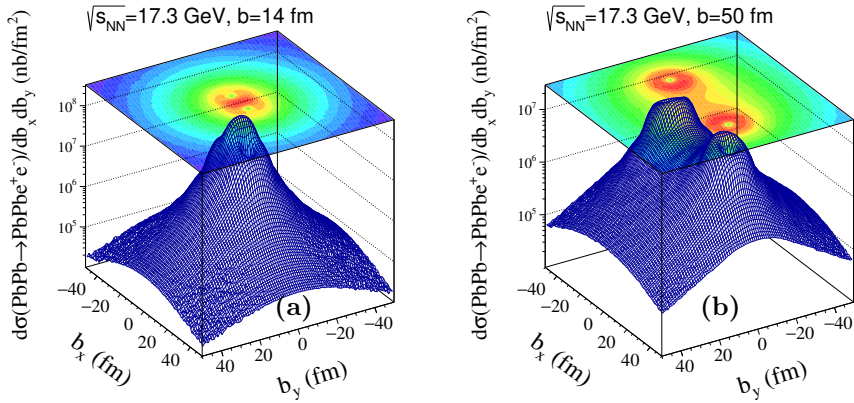


Fig. 7 Two-dimensional cross section as a function of b_x and b_y for two values of impact parameter: (a) $b=14\pm0.05$ fm and (b) $b=50\pm0.05$ fm.

results are symmetric under the following replacements: $b_x \rightarrow -b_x$ or $b_y \rightarrow -b_y$.

Figure 7 compares the integrated cross section on reaction plane (b_x, b_y) for two impact parameters: (a) $b=14\pm0.05$ fm (when nuclei are close to each other) and (b) $b=50\pm0.05$ fm (when nuclei are well separated). The landscape reflects the position of the nuclei in the moment of the closest approach. Similar plots have also been done for higher $\sqrt{s_{NN}}$ but the shape is almost unchanged, only the cross section value is different. This figure illustrates the influence of the geometry of the reaction. Regardless of the impact parameter (b), distance between colliding nuclei, the cross-section has a maximum at $b_x = 0$. The change of b is correlated with the shift in a peak at b_x .

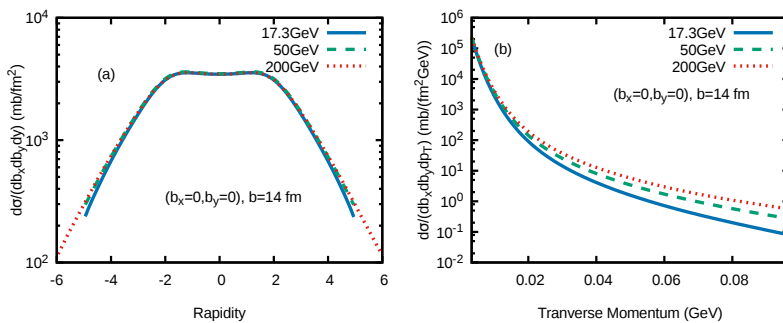


Fig. 8 (Color on-line) The differential cross section for various emission points of electrons in the $^{208}\text{Pb}+^{208}\text{Pb}$ reaction at $\sqrt{s_{NN}} = 17.3, 50, 200$ GeV at impact parameter 14 ± 0.05 fm.

The calculations confirm that the shape of the electron/positron distribution, shown in Fig. 8 does not depend on the energy of the colliding nuclei. There are visible small differences in the magnitude of cross sections for

$\sqrt{s_{NN}} = 17.3$ and 200 GeV at least in the selected limited $p_T=(0, 0.1)$ GeV range. Dependence on the rapidity is even weaker as the differences are visible only for $y > 3$.

These cross sections are used as weights in calculation of electromagnetic effects between electrons/positrons and the fast moving nuclei. The corresponding matrix has following dimensions: $b_{x,y}=(-50 \text{ fm}, 50 \text{ fm})$ - 99×99 points in the reaction plane and 100×15 in the (y, p_T) space.

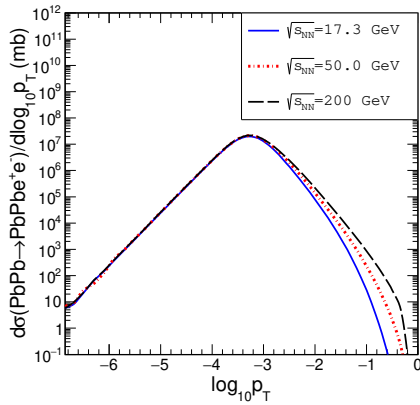


Fig. 9 Distribution of the cross section in $\log_{10} p_T$ for different energies: $\sqrt{s_{NN}} = 17.3$, 50 and 200 GeV (from bottom to top).

Rather small transverse momenta enter such calculation. To illustrate this in Fig. 9 we show a distribution in $\log_{10}(p_T)$. As seen from the figure the cross section is integrable and we have no problem with this with our Monte Carlo routine [56].

4 Electromagnetic interaction effects

It is our aim to study the influence of the strong EM fields on the distributions of produced electrons or positrons, separately for electrons and positrons.

The spectator system are modeled as two uniform spheres in their respective rest frames that change into disks in the overall center-of-mass collision frame. The total charge of nuclei is 82 consistent with UPC. The lepton emission region is reduced to a single point and the time of emission is a free parameter.

In this work we assume there is no delay time between collisions of nuclei and the start of the EM interactions. The z -dependence of the first occurrence of the e^+e^- pair is beyond the EPA and is currently not known. In our opinion production of e^+e^- happens when the moving cones, fronts of the EM fields,

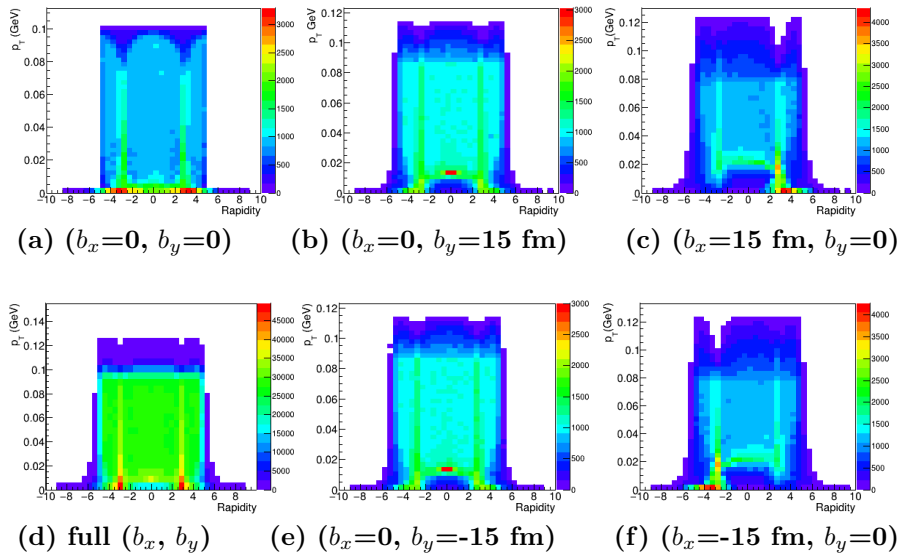


Fig. 10 (Color on-line) Rapidity vs p_T distributions for final (subjected to EM effects) electrons for different emission points: (a) (0, 0) and (d) full xy plane; (b) (0, 15 fm); (c) (15 fm, 0); (e) (0, -15 fm) and (f) (-15 fm, 0). These results are for $\sqrt{s_{NN}} = 17.3$ GeV.

cross each other. This happens for $z \approx 0$. In the following we assume $z = 0$ for simplicity.³

The trajectories of e^\pm in the field of moving nuclei are obtained by solving the equation of motion numerically for electrons/positrons:

$$\frac{d\vec{p}_{e^\pm}}{dt} = \vec{F}_{1,e^\pm}(\vec{r}_1, t) + \vec{F}_{2,e^\pm}(\vec{r}_2, t) . \quad (3)$$

The total interaction is a superposition of interactions with both nuclei which positions depend on time. We solve the motion of electron/positron in the overall center of mass system, i.e. both position and time are given in this frame. In this frame we have to deal with both electric and magnetic force [1]. Because nuclei are very heavy compared to electrons/positron their motion is completely independent and is practically not distorted by the EM interaction. We take:

$$\begin{aligned} \vec{r}_1(t) &= +\hat{z}ct + \vec{b}/2 , \\ \vec{r}_2(t) &= -\hat{z}ct - \vec{b}/2 , \end{aligned} \quad (4)$$

i.e. assume that the nuclei move along straight trajectories independent of the motion of electron/positron. The step of integration depends on energy and must be carefully adjusted.

³Any other distribution could be taken.

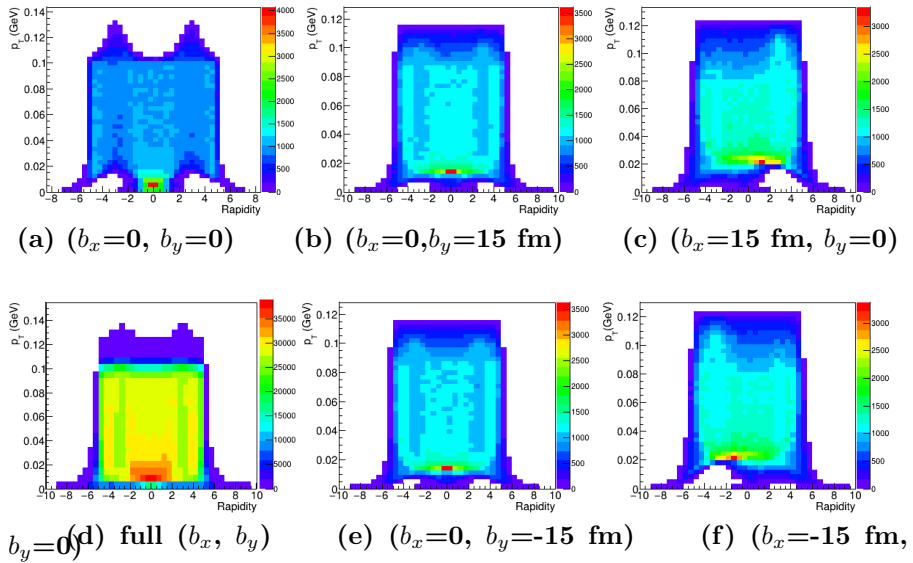


Fig. 11 (Color on-line) Rapidity vs p_T distributions for final (subjected to EM effects) positrons for different emission points: (a) (0, 0) and (d) full xy plane; (b) (0, 15 fm); (c) (15 fm, 0); (e) (0, -15 fm) and (f) (-15 fm, 0). These results are for $\sqrt{s_{NN}} = 17.3$ GeV.

Our approach can also be used to study the influence on the observables related to the dilepton pair, such as invariant mass or transverse momentum of the pair. Temporary calculation shows that the effect then is much smaller than for individual distributions. Therefore we decided not to discuss this in this paper.

The rapidity vs p_T distributions of initial leptons are obtained by randomly choosing the position on the two-dimensional space. The path of particle in electromagnetic field generated by nuclei are traced up to 10 000 fm away from the original interaction point. The Monte Carlo method is used to randomize the initial rapidity and p_T from uniform distribution. The initial rapidity and p_T of electrons/positrons are randomly chosen in the range: $y=(-5,5)$ and $p_T=(0, 0.1)$ GeV as fixed in the previous section. The (y, p_T) distributions for final (subjected to the EM evolution) leptons are presented in Fig. 10 for electrons and in Fig. 11 for positrons. These distributions were obtained by analyzing the EM evolution event-by-event. The number of events taken here is $n_{event} = 10^7$ for each two-dimensional plot.

For electron production an enhancement and for positron a loss with respect to the neighborhood or/and flat initial distribution is observed for $y \approx \pm 3$. This corresponds to the beam rapidity at $\sqrt{s_{NN}}=17.3$ GeV energy.

These two sets of two-dimensional plots illustrate effect of the EM interaction between e^+ or e^- and the moving nuclei. The motion of particles in the EM field of nuclei changes the initial conditions and the final (y, p_T) are slightly different. Fig. 10 shows the behavior of electrons and Fig. 11 of positrons at

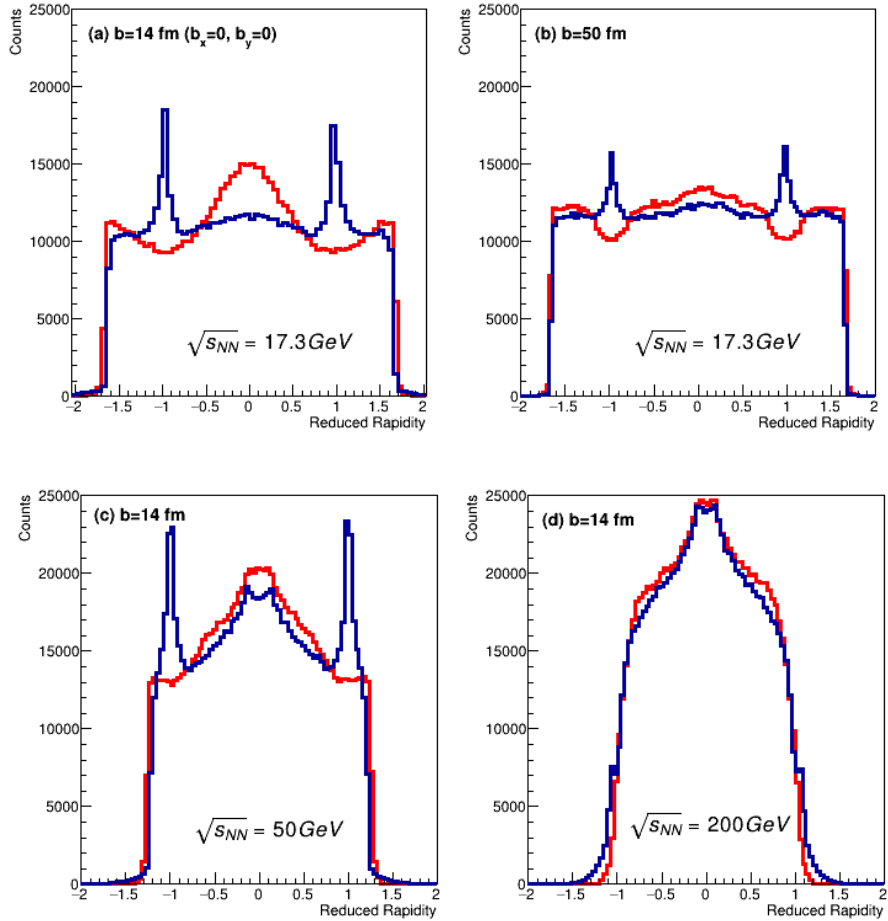


Fig. 12 (Color on-line) Reduced rapidity distributions for final electrons (blue) and positrons (red) for fixed b and ($b_x=0, b_y=0$) plane of emission points at three collision energies: $\sqrt{s_{NN}}=17.3, 50$ and 200 GeV.

CM (a) and different impact parameter points: (panels c,f) (± 15 fm, 0) and (panels b,e) (0, ± 15 fm) marked in Fig. 2. We observe that the maximal number of electrons is located where the cross section for positrons has minimum. The Coulomb influence is well visible as a missing areas for positrons for $p_T < 0.02$ GeV for particles emitted from the CM point. The emission of leptons from $b_y = \pm 15$ fm gives lower effect. The asymmetry in emission is well visible for $b_x = \pm 15$ fm, where a larger empty space is for positive rapidity when $b_x = 15$ fm and for negative rapidity when $b_x = -15$ fm.

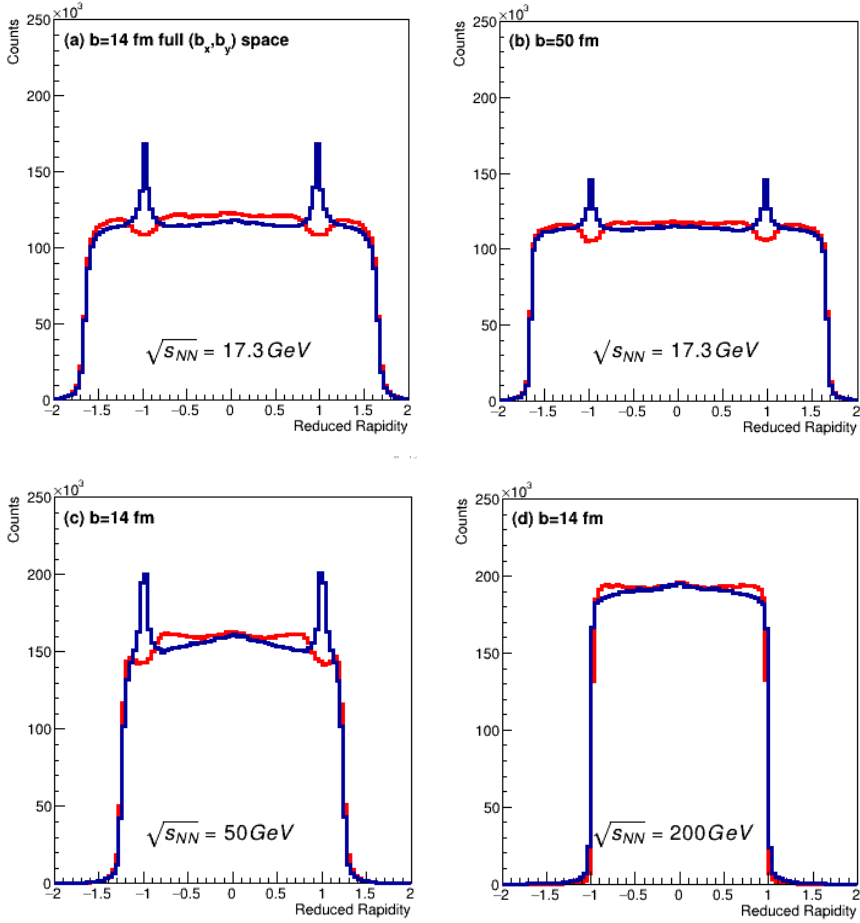


Fig. 13 (Color on-line) Reduced rapidity distributions for final electrons (blue) and positrons (red) for fixed b and full (b_x, b_y) plane of emission points at three collision energies: $\sqrt{s_{NN}}=17.3, 50$ and 200 GeV.

Although the EM effects are noticeable for electrons/positrons in different impact parameter points, the integration over full reaction plane washes out almost totally this impact.

For comparison the results of integration over full space $b_x=(-50$ fm, 50 fm) and $b_y=(-50$ fm, 50 fm) are shown in panels (d) of Figs. 10 and 11. These results are independent of the source of leptons, thus it could be treated as a general trend and an indication for which rapidity-transverse momentum ranges one could observe effects of the EM interaction between leptons and nuclei.

The distribution in reduced rapidity of final leptons are shown in Fig. 12 and 13. The reduced rapidity (dimensionless quantity) is the rapidity y

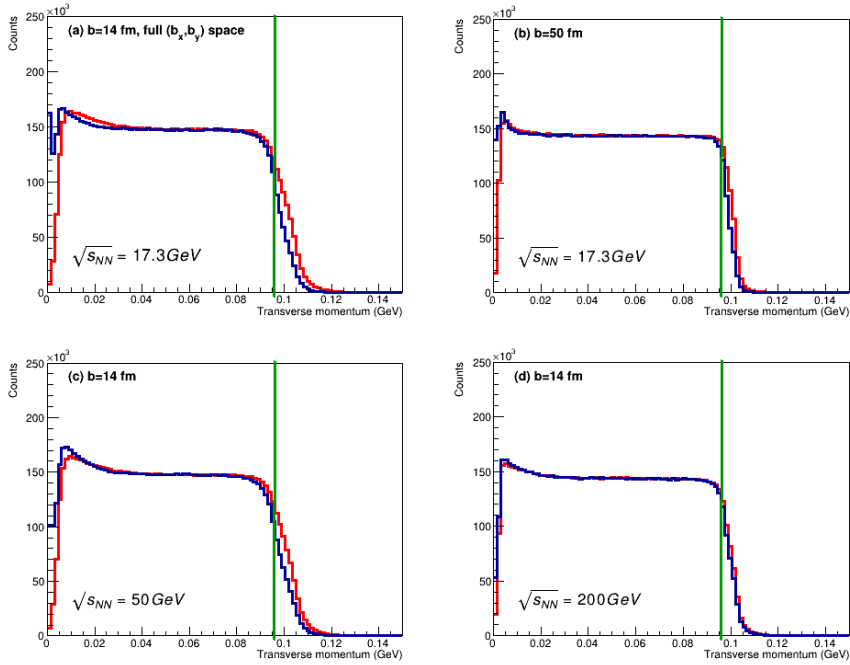


Fig. 14 (Color on-line) Transverse momentum distributions for final electrons (blue) and positrons (red) for fixed b and full (b_x, b_y) plane of emission points at three collision energies: $\sqrt{s_{NN}}=17.3, 50$ and 200 GeV.

normalized to the beam rapidity y_{beam} (different for various collision energies)

$$y_{red} = y/y_{beam} , \quad (5)$$

where

$$y_{beam} = \pm \ln \left(\frac{\sqrt{s_{NN}}}{m_p} \right) \quad (6)$$

and m_p is the proton mass. The results shown above were obtained, somewhat arbitrarily, with uniform distribution in (y, p_T) . This leads to the observation of peaks or dips at beam rapidities. No such peaks appear for $\sqrt{s} = 200$ GeV as here the chosen range of rapidity $(-5, 5)$ is not sufficient. Whether such effects survive when weighting with the b-space EPA cross section will be discussed below.

Fig. 12 is focused on emission from the center of mass point and Fig. 13 is obtained when integrating over full (b_x, b_y) plane. The main differences between electron (blue lines) and positron (red lines) distributions are not only at midrapidities but also around the beam rapidity. The effect is more visible for the CM emission point but it is slightly smoothed out when the full (b_x, b_y) plane is taken into consideration. Moreover increasing the impact parameter (panels (a) and (b)) diminishes the difference between rapidity distributions of

final electrons and positrons. The beam energy is another crucial parameter. The collision with $\sqrt{s_{NN}} > 100$ GeV (panel (d)) does not allow for sizeable effects of electromagnetic interaction between leptons and nuclei, at least at midrapidities.

The discussion of the EM interaction between e^+e^- and nuclei has to be completed by combining with the cross section of lepton production as obtained within EPA. Taking into account the leptons coming from photon-photon fusion the distributions from Fig. 10 and 11 are multiplied by differential cross section obtained with Eq.(2).

The details of the method are presented in Ref. [1] and adapted here from pion emission to electron/positron emission. In Fig. 14 we show the influence

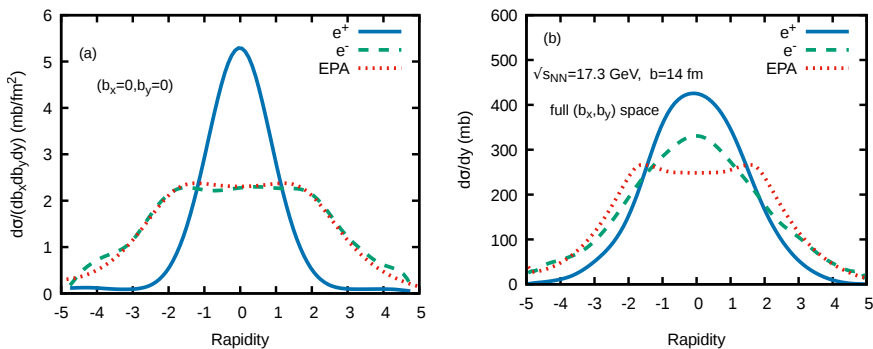


Fig. 15 (Color on-line) The electron and positron emission cross section normalized to 100% in the $^{208}\text{Pb}+^{208}\text{Pb}$ reaction at 158 GeV/nucleon energy ($\sqrt{s_{NN}} = 17.3$ GeV) at impact parameter 14 ± 0.05 fm assuming the $p_T=(0, 0.1)$ GeV produced in the center of mass (0, 0) point (a) and when integrating over full reaction space (b). Shown are original EPA distributions (dotted line) and results when including evolution in the EM field of nuclei for positrons (solid line) and for electrons (dashed line).

of EM interaction on p_T distributions. Here we integrate over rapidity and (b_x, b_y) . One can observe that the EM effects lead to a diffusion of transverse momenta (see the diffused edge at $p_T = 0.1$ GeV, marked by green vertical line). No spectacular influence is observed when changing the impact parameter or beam energy.

Fig. 15 shows a comparison of rapidity distribution of final electrons and positrons, assuming the particles are emitted from (a) the center of mass (0, 0) point and (b) when integrating over b_x, b_y . The comparison is done between EPA distribution relevant for initial stage (red, dotted line) with the final stage, resulting from the EM interaction of charged leptons with positively charged nuclei. If leptons are produced in the CM point, the electron distributions are almost unchanged but positron distributions are squeezed to $y < 2$. If the cross section is integrated over full (b_x, b_y) parameter space, the positron distribution is still steeper than that for electrons but mainly for $y < 2$.

Even when the leptons produced in the full (b_x, b_y) plane are considered, the e^+ and e^- distributions are different from the initial ones. The electrons under the EM interactions are focused at midrapidities.

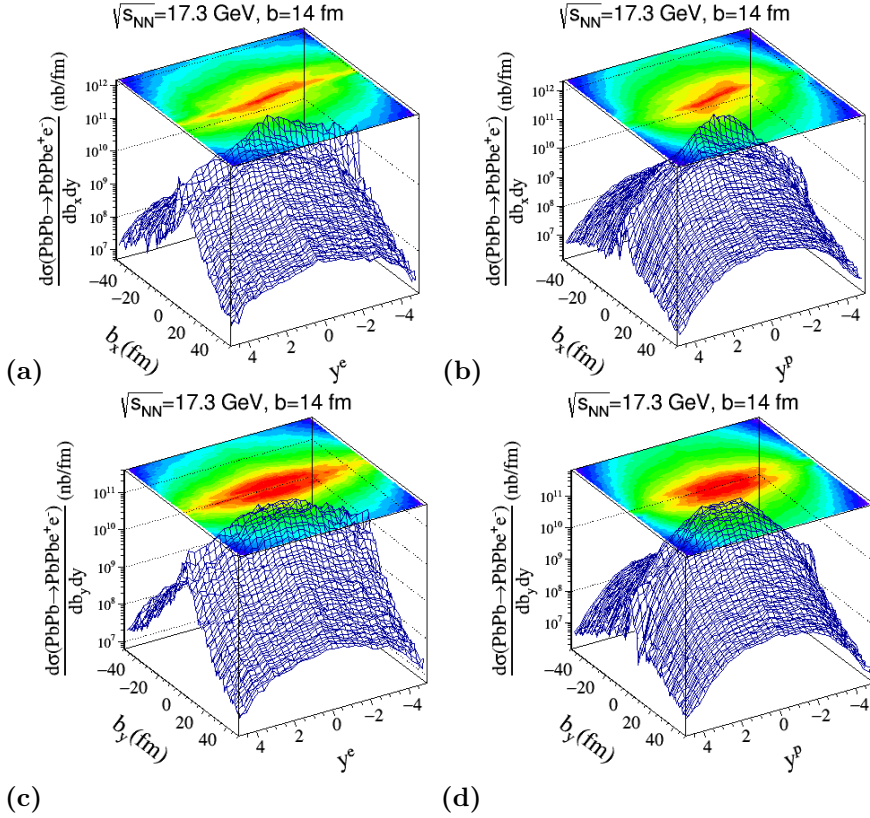


Fig. 16 Distribution of electrons ((a), (c)) and positrons ((b), (d)) for $\sqrt{s_{NN}} = 17.3$ GeV at $b=14$ fm integrated over $(b_x, b_y) = (-50 \text{ fm}, 50 \text{ fm})$, $p_T^{ini} = (0, 0.1 \text{ GeV})$

The dependence on the position of emission and final rapidity allows to understand how the geometry influences the electromagnetic interaction between leptons and nuclei. Figures 16, 17 and 18 present the cross section distribution in b_x (top rows) and rapidity for electrons (a) and positrons (b) and (bottom rows) b_y and rapidity for electrons (c) and positrons (d). Figs. 16 and 17 are for $\sqrt{s_{NN}} = 17.3$ GeV but with the impact parameter 14 ± 0.05 and 50 ± 0.05 fm. Fig. 18 is for $\sqrt{s_{NN}} = 200$ GeV and $b=14$ fm. These plots allow to investigate the anisotropy caused by the interaction between leptons and nuclei. It is more visible for larger impact parameter when the spectators are well separated (Fig. 17).

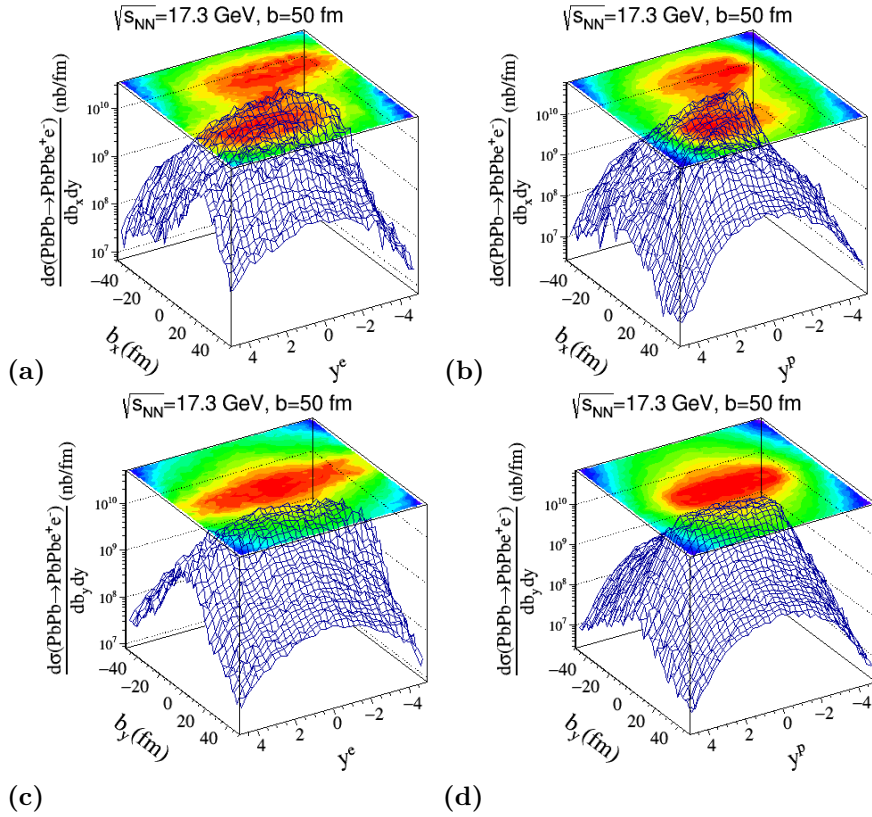


Fig. 17 Distribution of electrons ((a), (c)) and positrons ((b), (d)) for $\sqrt{s_{NN}} = 17.3$ GeV at $b=50$ fm integrated over $(b_x, b_y) = (-100 \text{ fm}, 100 \text{ fm})$, $p_T^{ini} = (0, 0.1 \text{ GeV})$.

Distributions for fixed impact parameter and different beam energies reflect the behavior seen in Fig. 13. For collision with $\sqrt{s_{NN}} = 200$ GeV (Fig. 18) the electrons and positrons almost do not feel the presence of the EM fields of the nuclei.

Integrating over full (b_x, b_y) plane one obtains the rapidity distribution of final leptons shown in Fig. 19 (a) separately for electrons and (b) positrons, for two impact parameters: 14 fm (full lines) and 50 fm (dashed lines). Electrons have a somewhat wider distribution than positrons and this is independent of the impact parameter. While positron rapidity distributions only weakly depend on collision energy it is not the case for electrons, where sizeable differences can be observed.

The ratio of distributions for positrons and electrons (Fig. 20) reflects the behavior seen in Figs. 16 and 17. This plot shows a combined effect of EPA cross section and the EM interactions of leptons with nuclei. Thus despite the production cross section is lower for larger impact parameter, the discussed phenomenon should be visible for larger rapidities. The ratio quickly changes

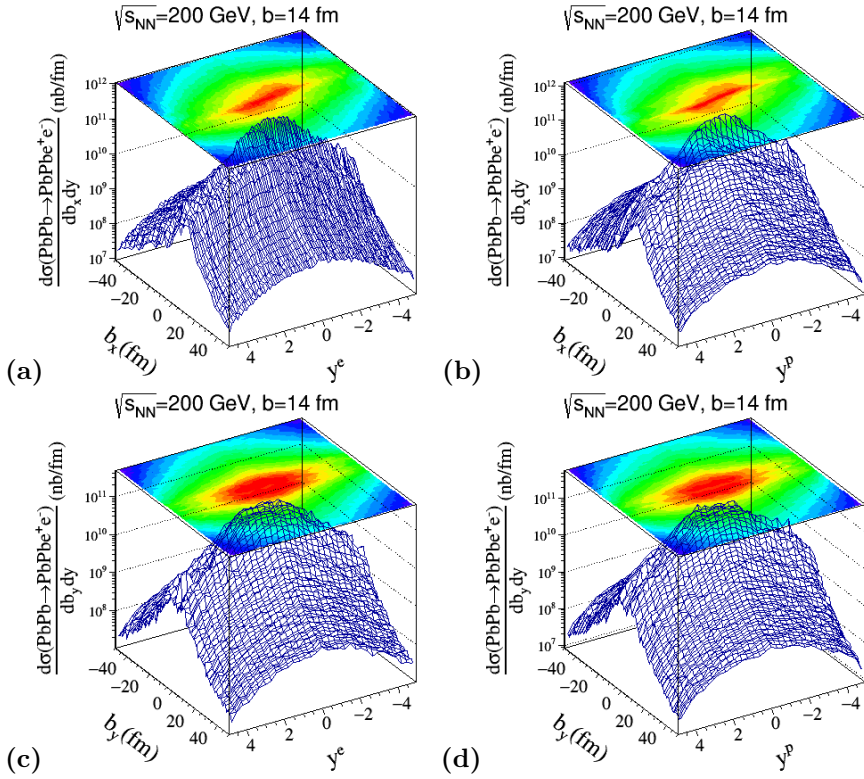


Fig. 18 Distribution of electrons ((a), (c)) and positrons ((b), (d)) for $\sqrt{s_{NN}} = 200$ GeV at $b=14$ fm integrated over $(b_x, b_y) = (-50 \text{ fm}, 50 \text{ fm})$ for $p_T^{ini} = (0, 0.1 \text{ GeV})$

with energy and tends to 1 for larger energies (see dotted line for $\sqrt{s_{NN}} = 200$ GeV).

Finally, we wish to make a supplementary comment on applicability of the classical approach used in the present paper. In principle, one could worry about uncertainty principle. In our calculations we assume that we know simultaneously momenta and positions of electrons/positrons. In the region of interest momenta of electrons/positrons are not small. Only transverse momenta are small. As shown in our paper, for the EM interactions the exact position is not crucial for final distributions. The effect becomes smaller only when the initial distances are dramatically modified. So we feel the uncertainty principle is not a crucial limitation for our study. In addition, we showed in our earlier calculations for pion production [1, 6] that the dramatic effects for pion velocities close to the velocity of one of the heavy ion beams can be well described by the classical approach.

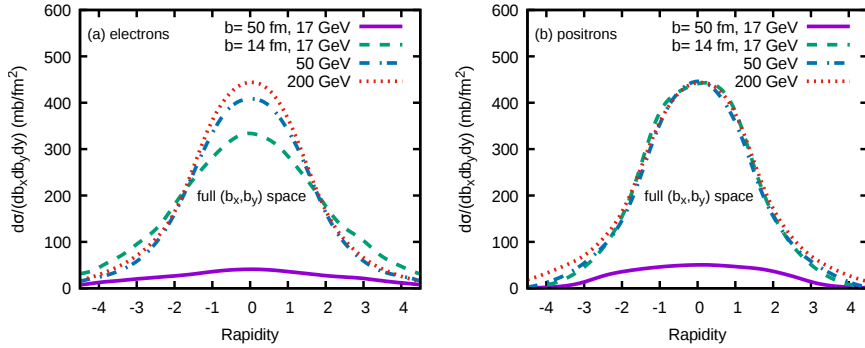


Fig. 19 Rapidity distribution of electrons for $\sqrt{s_{NN}} = 17.3$ GeV ($b=14$ fm, 50 fm) and 50 GeV and 200 GeV with $b=14 \pm 0.05$ fm (only) integrated over $(b_x, b_y)=(-50$ fm, 50 fm), $p_T^{ini}=(0, 0.1$ GeV).

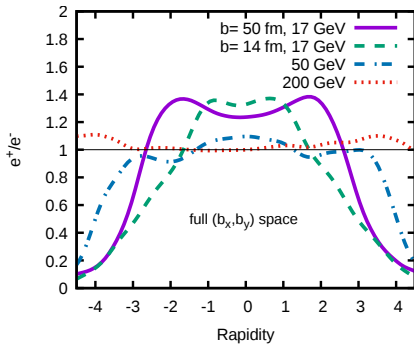


Fig. 20 The ratio of rapidity distributions of positrons and electrons for $\sqrt{s_{NN}} = 17.3$ GeV and fixed $b=14$ fm and 50 fm and $\sqrt{s_{NN}} = 50$ GeV and 200 GeV with fixed $b=14$ fm integrated over $(b_x, b_y)=(-50$ fm, 50 fm) and transverse momenta in the interval $p_T^{ini}=(0, 0.1$ GeV).

5 Conclusions

In the last 15 years the electromagnetic effects due to a large (moving) charge of the spectators on charged pion momentum distributions were observed both in theoretical calculations and experimentally in peripheral heavy ion collisions at SPS and RHIC energies. Interesting and sometimes spectacular effects were identified.

In the present paper we have discussed whether such effects could also be observed for the distributions of electrons/positrons produced via photon-photon fusion in heavy ion UPCs. The corresponding cross section can be rather reliably calculated and turned out to be large, especially for low transverse momentum electrons/positrons. The impact parameter equivalent photon approximation is well suitable for investigating the electromagnetic

effects. On the experimental side only rather large transverse momentum electrons/positrons could be measured so far at RHIC and the LHC, typically larger than 0.5 GeV.

We have organized calculations that include the EM effects using as an input EPA distributions. First multi-differential (in momenta and impact parameter) distributions for the diphoton production of the e^+e^- pairs are prepared in the impact parameter equivalent photon approximation. Such distributions are used next to calculate the propagation of the electrons/positrons in strong EM fields generated by the quickly moving nuclei. The propagation has been done by solving numerically relativistic equation of motion. Strong EM effects have been observed only at very small transverse momenta of electron/positron. Therefore to accelerate calculations we have limited to really small initial transverse momenta $p_T < 0.1$ GeV.

The shape of the differential cross section in rapidity and transverse momentum does not depend on the energy of the process but rather on the emission point in the impact parameter plane (b_x, b_y). We have investigated effects for different initial conditions, i.e. different emission positions in the impact parameter space.

The leptons interact electromagnetically with charged nuclei which changes their trajectories. The biggest effect has been identified for the CM emission point. However, the integration over full (b_x, b_y) plane washes out this effect to large extent. The range of $p_T=(0, 0.02$ GeV) has turned out the most preferable to investigate the influence of the EM effects on leptons originating from various (b_x, b_y) plane points.

Moreover, the impact parameter influences not only the value of the cross section but also the shapes of distributions of final leptons.

The $AA \rightarrow AAe^+e^-$ process creates leptons in a broad range of rapidities. We have found that only at small transverse momenta of electrons/positrons one can observe sizeable EM effects.

The performed calculations allow to conclude that the maximal beam energy for the Pb+Pb collision, where the EM effects between leptons and nuclei are evident at midrapidities, is probably $\sqrt{s_{NN}}=100$ GeV. Observation of this outcome at higher energies may be therefore rather difficult, if not impossible. The effect survives even at high energies but close to beam rapidity. However, this region of the phase space is usually not instrumented and does not allow electron/positron measurement.

So far the effect of EM interaction was studied for fixed values of the impact parameter (mainly for $b = 14$ fm). However, the impact parameter cannot be measured. The integration over the impact parameter is rather difficult and goes beyond the scope of the present paper. Such an integration will be studied elsewhere.

Our exploratory calculations have been done using impact parameter EPA. The discussed here final state electromagnetic effects were found at relatively small transverse momenta where more refined approach, including impact parameter-momentum correlations, may be necessary. Here we have discussed

the differences of the approach only for the production cross-section. Combining the FSI results and impact parameter - momentum correlations is difficult but could be done provided there is a chance to see the FSI effects experimentally.

On the experimental side a good measurement of electrons and positrons at low transverse momenta ($p_T < 0.1$ GeV) is necessary to see an effect. In principle, the measurement of the e^+/e^- ratio as a function of lepton rapidity and transverse momentum would be useful in this context. According to our knowledge there are definite plans only for high energies (ALICE-3 project) where, however, the EM effect should be very small (high collision energy). At CERN SPS energies the effect is rather large but at very small transverse momenta. RHIC would probably be a good place to observe the effect of the discussed here EM interactions but this would require a modification of the present apparatus.

The discussed here effects could be interesting in future at the AFTER@LHC experiment [57, 58], where $\sqrt{s_{NN}} \sim 100$ GeV. It may be also interesting to consider in future the problem in a quantal/field-theoretical approaches, but this is not a easy task.

Acknowledgement

A.S. is indebted to Andrzej Rybicki for past collaboration on electromagnetic effects in heavy ion collisions and Wolfgang Schäfer for a discussion on quantal effects. This work is partially supported by the Polish National Science Centre under Grant No. 2018/31/B/ST2/03537 and by the Center for Innovation and Transfer of Natural Sciences and Engineering Knowledge in Rzeszów (Poland).

References

- [1] Rybicki, A., Szczurek, A.: The Spectator Electromagnetic Effect on Charged Pion Spectra in Peripheral Ultrarelativistic Heavy-Ion Collisions. *Phys. Rev. C* **75**, 054903 (2007) <https://arxiv.org/abs/nucl-th/0610036>. <https://doi.org/10.1103/PhysRevC.75.054903>
- [2] Rybicki, A., Szczurek, A.: Spectator induced electromagnetic effect on directed flow in heavy ion collisions. *Phys. Rev. C* **87**(5), 054909 (2013) <https://arxiv.org/abs/1303.7354> [nucl-th]. <https://doi.org/10.1103/PhysRevC.87.054909>
- [3] Rybicki, A.: Strong and electromagnetic interactions at SPS energies. *PoS EPS-HEP2009*, 031 (2009). <https://doi.org/10.22323/1.084.0031>
- [4] Schlagheck, H.: Thermalization and flow in 158-GeV/A Pb + Pb collisions. *Nucl. Phys. A* **663**, 725–728 (2000) <https://arxiv.org/abs/nucl-ex/9909005>. [https://doi.org/10.1016/S0375-9474\(99\)00703-4](https://doi.org/10.1016/S0375-9474(99)00703-4)

- [5] Rybicki, A., Szczurek, A.: Charge splitting of directed flow and space-time picture of pion emission from the electromagnetic interactions with spectators (2014) <https://arxiv.org/abs/{1405.6860}> [nucl-th]
- [6] Ozvenchuk, V., Rybicki, A., Szczurek, A., Marcinek, A., Kielbowicz, M.: Spectator induced electromagnetic effects in heavy-ion collisions and space-time-momentum conditions for pion emission. *Phys. Rev. C* **102**(1), 014901 (2020) <https://arxiv.org/abs/1910.04544> [nucl-th]. <https://doi.org/10.1103/PhysRevC.102.014901>
- [7] Klusek-Gawenda, M., Szczurek, A.: Double scattering production of two positron–electron pairs in ultraperipheral heavy-ion collisions. *Phys. Lett. B* **763**, 416–421 (2016) <https://arxiv.org/abs/1607.05095> [nucl-th]. <https://doi.org/10.1016/j.physletb.2016.10.079>
- [8] van Hameren, A., Klusek-Gawenda, M., Szczurek, A.: Single- and double-scattering production of four muons in ultraperipheral *PbPb* collisions at the Large Hadron Collider. *Phys. Lett. B* **776**, 84–90 (2018) <https://arxiv.org/abs/1708.07742> [hep-ph]. <https://doi.org/10.1016/j.physletb.2017.11.029>
- [9] Dirac, P.A.M.: On the annihilation of electrons and protons. *Mathematical Proceedings of the Cambridge Philosophical Society* **26**(3), 361–375 (1930). <https://doi.org/10.1017/S0305004100016091>
- [10] Anderson, C.D.: The positive electron. *Phys. Rev.* **43**, 491–494 (1933). <https://doi.org/10.1103/PhysRev.43.491>
- [11] Breit, G., Wheeler, J.A.: Collision of two light quanta. *Phys. Rev.* **46**(12), 1087–1091 (1934). <https://doi.org/10.1103/PhysRev.46.1087>
- [12] Bethe, H.A., Heitler, W.: On the stopping of fast particles and on the creation of positive electrons. *Proc. R. Soc. Lond. A* **146**, 83–112 (1934). <https://doi.org/10.1098/rspa.1934.0140>
- [13] Landau, L.D., Lifshitz, E.: On the production of electrons and positrons by a collision of two particles. *Phys. Z. Sowjet.* **6**, 244 (1934). <https://doi.org/10.1103/PhysRevA.69.022708>
- [14] Williams, E.: Production of Electron-Positron Pairs. *Nature* **135**, 66 (1935). <https://doi.org/10.1038/135066a0>
- [15] Hubbell, J.H.: Electron–positron pair production by photons: A historical overview. *Radiation Physics and Chemistry* **75**(6), 614–623 (2006). <https://doi.org/10.1016/j.radphyschem.2005.10.008>. Pair Production
- [16] Ruffini, R., Vereshchagin, G., Xue, S.-S.: Electron-positron pairs in

- physics and astrophysics: from heavy nuclei to black holes. *Phys. Rept.* **487**, 1–140 (2010) <https://arxiv.org/abs/0910.0974> [astro-ph.HE]. <https://doi.org/10.1016/j.physrep.2009.10.004>
- [17] Khusek-Gawenda, M., Szczurek, A.: Exclusive muon-pair productions in ultrarelativistic heavy-ion collisions – realistic nucleus charge form factor and differential distributions. *Phys. Rev. C* **82**, 014904 (2010) <https://arxiv.org/abs/1004.5521> [nucl-th]. <https://doi.org/10.1103/PhysRevC.82.014904>
- [18] Kłusek-Gawenda, M., Ciemała, M., Schäfer, W., Szczurek, A.: Electromagnetic excitation of nuclei and neutron evaporation in ultrarelativistic ultraperipheral heavy ion collisions. *Phys. Rev. C* **89**(5), 054907 (2014) <https://arxiv.org/abs/1311.1938> [nucl-th]. <https://doi.org/10.1103/PhysRevC.89.054907>
- [19] Adams, J., *et al.*: Production of e^+e^- pairs accompanied by nuclear dissociation in ultra-peripheral heavy ion collision. *Phys. Rev. C* **70**, 031902 (2004) <https://arxiv.org/abs/nuclex/0404012>. <https://doi.org/10.1103/PhysRevC.70.031902>
- [20] Adam, J., *et al.*: Low- p_T e^+e^- pair production in Au+Au collisions at $\sqrt{s_{NN}} = 200$ GeV and U+U collisions at $\sqrt{s_{NN}} = 193$ GeV at STAR. *Phys. Rev. Lett.* **121**(13), 132301 (2018) <https://arxiv.org/abs/1806.02295> [hep-ex]. <https://doi.org/10.1103/PhysRevLett.121.132301>
- [21] Aaboud, M., *et al.*: Observation of centrality-dependent acoplanarity for muon pairs produced via two-photon scattering in Pb+Pb collisions at $\sqrt{s_{NN}} = 5.02$ TeV with the ATLAS detector. *Phys. Rev. Lett.* **121**(21), 212301 (2018) <https://arxiv.org/abs/1806.08708> [nucl-ex]. <https://doi.org/10.1103/PhysRevLett.121.212301>
- [22] Aad, G., *et al.*: Exclusive dimuon production in ultraperipheral Pb+Pb collisions at $\sqrt{s_{NN}} = 5.02$ TeV with ATLAS. *Phys. Rev. C* **104**, 024906 (2021) <https://arxiv.org/abs/2011.12211> [nucl-ex]. <https://doi.org/10.1103/PhysRevC.104.024906>
- [23] Khusek-Gawenda, M., Rapp, R., Schäfer, W., Szczurek, A.: Dilepton Radiation in Heavy-Ion Collisions at Small Transverse Momentum. *Phys. Lett. B* **790**, 339–344 (2019) <https://arxiv.org/abs/1809.07049> [nucl-th]. <https://doi.org/10.1016/j.physletb.2019.01.035>
- [24] Li, C., Zhou, J., Zhou, Y.-J.: Probing the linear polarization of photons in ultraperipheral heavy ion collisions. *Phys. Lett. B* **795**, 576–580 (2019) <https://arxiv.org/abs/1903.10084> [hep-ph]. <https://doi.org/10.1016/j.physletb.2019.07.005>

- [25] Zha, W., Brandenburg, J.D., Tang, Z., Xu, Z.: Initial transverse-momentum broadening of Breit-Wheeler process in relativistic heavy-ion collisions. *Phys. Lett. B* **800**, 135089 (2020) <https://arxiv.org/abs/1812.02820> [nucl-th]. <https://doi.org/10.1016/j.physletb.2019.135089>
- [26] Klein, S., Mueller, A.H., Xiao, B.-W., Yuan, F.: Lepton Pair Production Through Two Photon Process in Heavy Ion Collisions. *Phys. Rev. D* **102**(9), 094013 (2020) <https://arxiv.org/abs/2003.02947> [hep-ph]. <https://doi.org/10.1103/PhysRevD.102.094013>
- [27] Wang, R.-j., Pu, S., Wang, Q.: Lepton pair production in ultraperipheral collisions. *Phys. Rev. D* **104**(5), 056011 (2021) <https://arxiv.org/abs/2106.05462> [hep-ph]. <https://doi.org/10.1103/PhysRevD.104.056011>
- [28] Khusek-Gawenda, M., Schäfer, W., Szczurek, A.: Centrality dependence of dilepton production via $\gamma\gamma$ processes from Wigner distributions of photons in nuclei. *Phys. Lett. B* **814**, 136114 (2021) <https://arxiv.org/abs/2012.11973> [hep-ph]. <https://doi.org/10.1016/j.physletb.2021.136114>
- [29] Khusek-Gawenda, M., Rapp, R., Schäfer, W., Szczurek, A.: Dilepton Radiation in Heavy-Ion Collisions at Small Transverse Momentum. *Phys. Lett. B* **790**, 339–344 (2019) <https://arxiv.org/abs/1809.07049> [nucl-th]. <https://doi.org/10.1016/j.physletb.2019.01.035>
- [30] Khusek-Gawenda, M., Schäfer, W., Szczurek, A.: Centrality dependence of dilepton production via $\gamma\gamma$ processes from Wigner distributions of photons in nuclei. *Phys. Lett. B* **814**, 136114 (2021) <https://arxiv.org/abs/2012.11973> [hep-ph]. <https://doi.org/10.1016/j.physletb.2021.136114>
- [31] Rybicki, A.: What Is the role of nuclear effects in ultrarelativistic reactions at 158-GeV/nucleon? *Acta Phys. Polon. B* **42**, 867–876 (2011). <https://doi.org/10.5506/APhysPolB.42.867>
- [32] Bethe, H.A., Maximon, L.C.: Theory of Bremsstrahlung and Pair Production. 1. Differential Cross Section. *Phys. Rev.* **93**, 768–784 (1954). <https://doi.org/10.1103/PhysRev.93.768>
- [33] Ivanov, D., Melnikov, K.: Lepton pair production by a high-energy photon in a strong electromagnetic field. *Phys. Rev. D* **57**, 4025–4034 (1998) <https://arxiv.org/abs/hep-ph/9709352>. <https://doi.org/10.1103/PhysRevD.57.4025>
- [34] Tuchin, K.: Multi-photon interactions in lepton photo-production on nuclei at high energies. *Phys. Rev. D* **80**, 093006 (2009) <https://arxiv.org/abs/0907.5189> [hep-ph]. <https://doi.org/10.1103/PhysRevD.80.093006>

- [35] Sun, Z.-h., Zheng, D.-x., Zhou, J., Zhou, Y.-j.: Studying Coulomb correction at EIC and EicC. *Phys. Lett. B* **808**, 135679 (2020) <https://arxiv.org/abs/2002.07373> [hep-ph]. <https://doi.org/10.1016/j.physletb.2020.135679>
- [36] Ivanov, D., Kuraev, E.A., Schiller, A., Serbo, V.G.: Production of e^+e^- pairs to all orders in $Z\alpha$ for collisions of high-energy muons with heavy nuclei. *Phys. Lett. B* **442**, 453–458 (1998) <https://arxiv.org/abs/hep-ph/9807311>. [https://doi.org/10.1016/S0370-2693\(98\)01278-7](https://doi.org/10.1016/S0370-2693(98)01278-7)
- [37] Lee, R.N., Milstein, A.I., Strakhovenko, V.M.: High-energy expansion of Coulomb corrections to the e^+e^- photoproduction cross-section. *Phys. Rev. A* **69**, 022708 (2004) <https://arxiv.org/abs/hep-ph/0310108>. <https://doi.org/10.1103/PhysRevA.69.022708>
- [38] Sandrock, A., Rhode, W.: Coulomb corrections to the bremsstrahlung and electron pair production cross section of high-energy muons on extended nuclei (2018) <https://arxiv.org/abs/{1807.08475}> [hep-ph]
- [39] Segev, B., Wells, J.C.: A Light fronts approach to electron - positron pair production in ultrarelativistic heavy ion collisions. *Phys. Rev. A* **57**, 1849 (1998) <https://arxiv.org/abs/physics/9710008>. <https://doi.org/10.1103/PhysRevA.57.1849>
- [40] Segev, B., Wells, J.C.: Exact Z^2 scaling of pair production in the high-energy limit of heavy ion collisions. *Phys. Rev. C* **59**, 2753–2756 (1999) <https://arxiv.org/abs/physics/9805013>. <https://doi.org/10.1103/PhysRevC.59.2753>
- [41] Eichmann, U., Reinhardt, J., Greiner, W.: Coulomb effects on electromagnetic pair production in ultrarelativistic heavy ion collisions. *Phys. Rev. A* **59**, 1223–1237 (1999) <https://arxiv.org/abs/nucl-th/9806031>. <https://doi.org/10.1103/PhysRevA.59.1223>
- [42] Ivanov, D.Y., Schiller, A., Serbo, V.G.: Large Coulomb corrections to the e^+e^- pair production at relativistic heavy ion colliders. *Phys. Lett. B* **454**, 155–160 (1999) <https://arxiv.org/abs/hep-ph/9809449>. [https://doi.org/10.1016/S0370-2693\(99\)00323-8](https://doi.org/10.1016/S0370-2693(99)00323-8)
- [43] Baltz, A.J., Gelis, F., McLerran, L.D., Peshier, A.: Coulomb corrections to e^+e^- production in ultrarelativistic nuclear collisions. *Nucl. Phys. A* **695**, 395–429 (2001) <https://arxiv.org/abs/nucl-th/0101024>. [https://doi.org/10.1016/S0375-9474\(01\)01109-5](https://doi.org/10.1016/S0375-9474(01)01109-5)
- [44] Lee, R.N., Milstein, A.I., Serbo, V.G.: Structure of the Coulomb and unitarity corrections to the cross-section of e^+e^- pair production in ultrarelativistic nuclear collisions. *Phys. Rev. A* **65**, 022102 (2002) <https://arxiv.org/abs/hep-ph/0105101>

- [org/abs/hep-ph/0108014](https://doi.org/10.1103/PhysRevA.65.022102). <https://doi.org/10.1103/PhysRevA.65.022102>
- [45] Baltz, A.J., McLerran, L.D.: Two center light cone calculation of pair production induced by ultrarelativistic heavy ions. *Phys. Rev. C* **58**, 1679–1688 (1998) <https://arxiv.org/abs/nuc1-th/9804042>. <https://doi.org/10.1103/PhysRevC.58.1679>
 - [46] Baltz, A.J.: Coulomb corrections in the calculation of ultrarelativistic heavy ion production of continuum e^+e^- pairs. *Phys. Rev. C* **68**, 034906 (2003) <https://arxiv.org/abs/nuc1-th/0305083>. <https://doi.org/10.1103/PhysRevC.68.034906>
 - [47] Bartos, E., Gevorkyan, S.R., Kuraev, E.A., Nikolaev, N.N.: Multiple lepton pair production in relativistic ion collisions. *Phys. Lett. B* **538**, 45–51 (2002) <https://arxiv.org/abs/hep-ph/0204327>. [https://doi.org/10.1016/S0370-2693\(02\)01991-3](https://doi.org/10.1016/S0370-2693(02)01991-3)
 - [48] Bartos, E., Gevorkyan, S.R., Kuraev, E.A., Nikolaev, N.N.: Multiple exchanges in lepton pair production in high-energy heavy ion collisions. *J. Exp. Theor. Phys.* **100**(4), 645–655 (2005) <https://arxiv.org/abs/hep-ph/0410263>. <https://doi.org/10.1134/1.1926426>
 - [49] Baur, G., Ferreira Filho, L.G.: COHERENT PARTICLE PRODUCTION AT RELATIVISTIC HEAVY ION COLLIDERS INCLUDING STRONG ABSORPTION EFFECTS. *Nucl. Phys. A* **518**, 786–800 (1990). [https://doi.org/10.1016/0375-9474\(90\)90191-N](https://doi.org/10.1016/0375-9474(90)90191-N)
 - [50] Bertulani, C.A., Klein, S.R., Nystrand, J.: Physics of ultra-peripheral nuclear collisions. *Ann. Rev. Nucl. Part. Sci.* **55**, 271–310 (2005) <https://arxiv.org/abs/nuc1-ex/0502005>. <https://doi.org/10.1146/annurev.nuc1.55.090704.151526>
 - [51] Baltz, A.J., Gorbunov, Y., Klein, S.R., Nystrand, J.: Two-Photon Interactions with Nuclear Breakup in Relativistic Heavy Ion Collisions. *Phys. Rev. C* **80**, 044902 (2009) <https://arxiv.org/abs/0907.1214> [nucl-ex]. <https://doi.org/10.1103/PhysRevC.80.044902>
 - [52] Klein, S.R., Nystrand, J., Seger, J., Gorbunov, Y., Butterworth, J.: STARlight: A Monte Carlo simulation program for ultra-peripheral collisions of relativistic ions. *Comput. Phys. Commun.* **212**, 258–268 (2017) <https://arxiv.org/abs/1607.03838> [hep-ph]. <https://doi.org/10.1016/j.cpc.2016.10.016>
 - [53] Vidovic, M., Greiner, M., Best, C., Soff, G.: Impact parameter dependence of the electromagnetic particle production in ultrarelativistic heavy ion collisions. *Phys. Rev. C* **47**, 2308–2319 (1993). <https://doi.org/10.1103/PhysRevC.47.2308>

- [54] Hencken, K., Trautmann, D., Baur, G.: Impact parameter dependence of the total probability for the electromagnetic electron - positron pair production in relativistic heavy ion collisions. Phys. Rev. A **51**, 1874–1882 (1995) <https://arxiv.org/abs/nucl-th/9410014>. <https://doi.org/10.1103/PhysRevA.51.1874>
- [55] Abbas, E., *et al.*: Charmonium and e^+e^- pair photoproduction at mid-rapidity in ultra-peripheral Pb-Pb collisions at $\sqrt{s_{\text{NN}}}=2.76$ TeV. Eur. Phys. J. C **73**(11), 2617 (2013) <https://arxiv.org/abs/1305.1467> [nucl-ex]. <https://doi.org/10.1140/epjc/s10052-013-2617-1>
- [56] Lepage, G.P.: A New Algorithm for Adaptive Multidimensional Integration. J. Comput. Phys. **27**, 192 (1978). [https://doi.org/10.1016/0021-9991\(78\)90004-9](https://doi.org/10.1016/0021-9991(78)90004-9)
- [57] Hadjidakis, C., *et al.*: A fixed-target programme at the LHC: Physics case and projected performances for heavy-ion, hadron, spin and astroparticle studies. Phys. Rept. **911**, 1–83 (2021) <https://arxiv.org/abs/1807.00603> [hep-ex]. <https://doi.org/10.1016/j.physrep.2021.01.002>
- [58] AFTER@LHC. <http://after.in2p3.fr/>